Original Article

Exploring the potential of Beta- 2 Agonist, Salbutamol Against Muscle Atrophy Using Computational Approach

Anand Kumar[1*], Priyanka Prajapati[1], Rohit Kumar[1], and Sapana Kushwaha[1]

[1*,2,3] Department of Pharmaceutical Sciences, School of Pharmaceutical Sciences, Babasaheb Bhimrao Ambedkar University, Vidya Vihar, Raebareli Road, Lucknow-226025 India

***Corresponding author:-** Anand Kumar

*Department of Pharmaceutical Sciences, School of Pharmaceutical Sciences, Babasaheb Bhimrao Ambedkar University, Vidya Vihar, Raebareli Road, Lucknow-226025 India. Email- anandkumarpharm@gmail.com; anandkmr.rs@bbau.ac.in
DOI: 10.47750/pnr.2022.13.S05.417

Abstract

Background: Muscle atrophy affects many individuals every year, and there are only a few FDA-approved drugs to treat skeletal muscle wasting. This is caused by a combination of factors including inactivity, aging, and a wide range of diseases such as diabetes, cancer, neurodegenerative disorders, bacterial and viral infections, chronic respiratory and renal diseases, and several drug side effects.

Aim: Therefore, the present study was aimed to evaluate the anti-muscle atrophy potential of existing beta 2 agonist, salbutamol through *in silico* approach.

Methods: Solubility analysis of salbutamol was performed in different solvents *i.e.* water, ethanol, ether, HCl, and chloroform to confirm the solubility behaviour. Calibration curve of salbutamol was prepared in 0.1N HCl (276 nm) and assessed by UV spectroscopy. Fourier transform infrared spectroscopy (FTIR) analysis of salbutamol was performed to confirm the purity of salbutamol. Furthermore, molecular docking was performed using the Autodock Vina software to confirm the affinity of ligand-protein complexes (AKT1, Growth differentiation factor 8 (GDF-8), IGF-1, MuRF-1, MyoD, and TNF-α).

Results: Solubility results showed that salbutamol was sparingly soluble in water and ether, freely soluble in 0.1 N HCl solutions, and also in ethanol and chloroform which indicates the drug is highly soluble. The calibration curve uses to assess the amount of drug in plasma a different time interval. FTIR results of salbutamol showed sharp peaks at 4000-400 cm^{-1} wavelengths. The molecular docking shows the high binding energy with the target protein *viz.* AKT1, Growth differentiation factor 8 (GDF-8), IGF-1, MuRF-1, MyoD, and TNF

Conclusions: Results demonstrate that β2-adrenergic agonist salbutamol shows good binding affinity to catabolic (MuRF-1, myostatin, MyoD and TNF-α) and anabolic proteins (AKT1, IGF-1, and GDF-8) through a computational approach to predict the skeletal muscle atrophy.

Keyboards: Skeletal muscle atrophy, Beta2-agonist, molecular docking, AKT1 and MuRF-1

INTRODUCTION

Skeletal muscle atrophy is a common illness condition caused by inactivity, aging, and diseases including sepsis, diabetes, cachexia and side effects of drugs (Cohen et al., 2015). Muscle mass and function loss ultimately affects the quality of life by increasing morbidity and mortality. Exercise, acupuncture has been recognised for anti-muscle atrophy measure to treat muscle wasting. The last ten years have seen a number of studies illuminate the underlying molecular pathways, opening the door to the development of new medications for muscle atrophy (Sartori et al., 2021). According to studies, the retrieval of both agonists and beta blockers performed exceptionally well when individual docking experiments were combined with receptor ensemble docking (Costanzi & Vilar, 2012). Based on predictions of the energy of the binding protein-ligand interactions and modes of action, pharmacological agents for different diseases could be screened using molecular docking. The targeted binding site of a protein is computationally modelled for ligand binding poses, and poses are then optimised to provide structural information and activity predictions in the form of thermodynamic binding affinities. The process of "reverse docking," in which a small molecule is docked across different potential protein targets, uses docking to uncover binding partners and drug mechanisms of action. In "one target, many compounds" approaches, docking was used to enrich for potential hit substances that bind pre-specified proteins (Meng et al., 2011). Salbutamol (SLB) is a short acting of synthetic selective to β2-adrenoceptors agonist traditionally used as bronchodilator for treatment of bronchial associated with asthma and symptomatic patients with COPD. SLB is similar chemical structure with of adrenaline derived by catecholamine act as neurotransmitter (Hostrup et al., 2018). As epinephrine and β2-agonists prevent protein degradation in isolated rat muscles, and showed direct

action in protecting skeletal muscle. (Elfellah et al., 1989). Furthermore, findings revealed that a selective 2-adrenoceptor stimulant causes smooth muscle relaxation *via* increased intracellular cyclic adenosine monophosphate (cAMP), which relaxes bronchial and uterine muscles, dilates peripheral vessels, and increases heart rate (Galaz-Montoya et al., 2017).

Negative regulators of skeletal muscle growth include myostatin (MSTN), which is highly conserved (Morissette et al., 2009). Findings also demonstrated that myostatin controls Akt's downstream effectors in the mTOR pathway to influence skeletal muscle hypertrophy (Morissette et al., 2009). Another important growth factor that controls the anabolic and catabolic pathways in skeletal muscle is insulin-like growth factor-1 (IGF-1). IGF-1 stimulates PI3K/Akt/mTOR and PI3K/Akt/GSK3 pathways, which both increase skeletal muscle protein synthesis (Yoshida & Delafontaine, 2020). Additionally, muscle wasting results in the activation of signalling pathways that are triggered by cytokines like IL-6, IL-1, TNF-alpha, IFN-gamma, and myostatin. Not only that, but TNF-alpha also activated the Atrogin1 and MuRF1, leading to proteolysis (Pijet et al., 2013). So, present study used a novel computational approach to compute the binding affinity of beta 2-adrenergic agonists, to targeted protein for skeletal muscle atrophy.

MATERIALS AND METHODS

Chemicals

Salbutamol was gifted from Cipla Pvt. Ltd, India. All the solvents and chemicals were used of analytical grades with 99% purity and in house distilled water was used for carrying the experiment.

Apparatus and procedures

The required amounts of water, ethanol, ether, HCl, and chloroform were combined with a volume fraction uncertainty of 0.001 to create the binary solvent mixtures. We had used a shaker in an incubator with a temperature-control system to equilibrate excess amounts of the solids in mixed solvents at 25 °C. The temperature was maintained constant to within 0.2 °C. (Savjani et al., 2012) and reading were taking by UV spectrophotometrically (V-530, UV-Vis spectrophotometer) at wavelengths of 225 and 276 nm for salbutamol (SLB). The calibration curves were used to determine the concentrations of the diluted solutions. The average of at least three repeated experiments is represented by each experimental data point.

Preparation of standard stock solution

In order to create working standard solutions with 20g/ml of SLB, a precisely weighed (2.0 mg) sample of pure SLB was dissolved in a 100 ml volumetric flask and diluted to the appropriate concentration with phosphate buffer (pH 7.4). (Guo et al., 2016).

Preparation of working standard solutions

From the aforementioned stock solution, desired concentrations were made by transferring a specific volume into separate 10 ml volumetric flasks and increasing the volume with phosphate buffer to 10 ml (Guo et al., 2016).

Determination of absorption maximas

Solutions containing 10 g/ml of salbutamol (SLB) were scanned in the 200–400 nm range against phosphate buffer (pH 7.4) as a blank after adequate dilution of standard solutions SLB with phosphate buffer (pH 7.4). Additionally, the overlapping spectra were gathered to determine the medication's maximum wavelength of absorption (276 nm max). The calibration curves were plotted to verify Beer's law (Guo et al., 2016).

Fourier transforms infrared spectroscopy (FTIR)

FTIR spectroscopy was used to investigate SLB. FT-IR was used to capture the spectra of a pure drug. KBr discs were used to prepare the samples (2 mg sample in 200 mg KBr). The resolution was 2 cm^{-1} and the scanning range was 400-4000 cm^{-1} (Grisedale et al., 2013).

Evaluation of protein model

Ramachandran plot analysis was used to evaluate of the protein structures using PROCHECK. The models were then analysed using ERRAT from the online web server https://saves.mbi.ucla.edu and ProSA from the online web server https://prosa.services.came.sbg.ac

Ligand-protein docking

The three-dimensional (3D) structure of the ligand (salbutamol) was obtained from Pub Chem (CID: 2083) (https://pubchem.ncbi.nlm.nih.gov) and the structures of AKT1, Growth differentiation factor 8 (GDF-8), IGF-1, MuRF-1, MyoD, and TNF-α were obtained from the RCSB PDB online web source (https://www.rcsb.org). Autodock Vina 1.2.0 was used to create this. Non-polar hydrogen atoms were fused in the protein, and the protein received a total Kollman and Gasteiger charge. It was determined that the protein had no unattached atoms. The ligand also received partial charges from Kollman and Gasteiger, and all torsions were permitted to rotate during docking. A grid box was created and around the active site to cover the entire protein binding site and allow ligands to move freely. This grid box was calculated by AutoGrid and contained the ligand and AKT1, GDF-8, IGF-1, MuRF-1, MyoD, and TNF- alpha (PDB ID: 6HHG, 5JI1, 1B9G4, 2D8U, and 3RT4). With default parameter settings, 100 runs of the Lamarckian genetic

algorithm were made. The interactions of ligands (AKT1, GDF-8, IGF-1, MuRF-1, MyoD, and TNF-α) in complex conformations were investigated, including hydrogen bonds and bond lengths. PyMOL and Biovia Discovery Studio are using visualisation tools (Meng et al., 2011).

RESULTS

Determination of salbutamol solubility

An excess amount of drug was taken in 2ml centrifuge tubes containing different solvents separately over rotaspin for 24 hr. The saturated solution was centrifuged at 5000 rpm for 20 min followed the measurement of the solubilized drug by UV Spectroscopy at 276 nm (Table 1).

Table 1: Experimental and predicted molar solubility of salbutamol in distilled water, ether, 0.1N HCl, ethanol and chloroform mixtures at 25° C.

S. No.	Solvents	Solubility
1	Distilled Water	Sparingly soluble
2	Ether	Slightly soluble
3	0.1NHCl	Freely Soluble
4	Ethanol	Soluble
5	Chloroform	Very soluble

Construction of standard graph of salbutamol:

The stock solution of salbutamol in 0.1N HCl was scanned at the range of 200-400 nm. The maximum absorbance was found at 276nm. The calibration curve of salbutamol was plotted in 0.1N HCl (Figure 1 and Table 2).

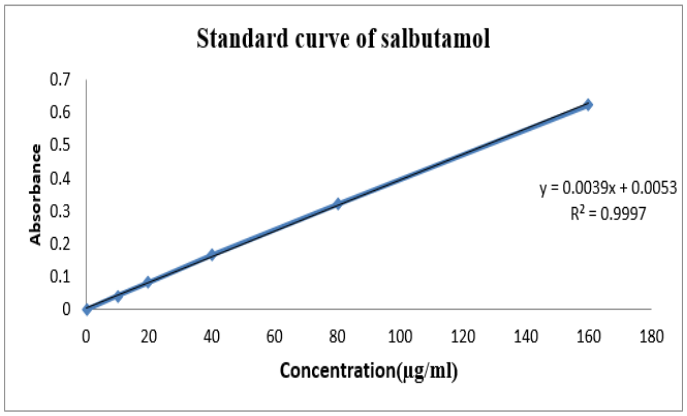

Figure 1: Standard graph of salbutamol in 0.1N HCl

Table 2: Standard values of salbutamol

S. No.	Concentration (µg/ml)	Absorbance at 276 nm
1	0	0
2	10	0.043
3	20	0.084
4	40	0.165
6	80	0.323
7	160	0.625

FTIR Spectral Analysis:

Salbutamol FTIR spectra revealed sharp peaks at the following wavelengths: 1409 cm^{-1} , - (OH) for bending & hydroxyl group, 1661 cm^{-1} - (C=C) for stretch & aromatic ring, 1100 cm^{-1} , (C-O) for stretch & ether group, 1028 cm^{-1} - (C-H) for bend, aromatic benzene ring, 3000 cm^{-1} , (C-H) for stretch & aldehyde, 1650 cm^{-1} - (C=C) for stretch and alkenes (Figure 2).

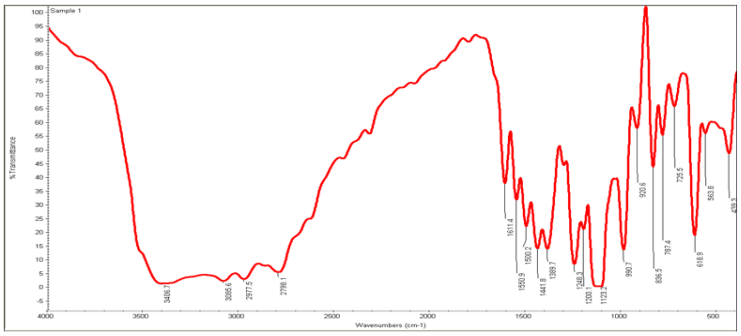

Figure 2: FTIR spectrum of pure salbutamol

Molecular docking and validation of protein models

The six protein models were evaluated using Ramachandran plot statistics analysis in PROCHECK by assessing the stereo-chemical quality of the protein structures on a residue-by-residue basis. The results showed that residues of all protein models in the AKT1, GDF-8, IGF-1, MuRF-1, MyoD, and TNF-α proteins showed that 92.8, 82.7, 67.3, 85.8, 95.2, and 89.9% of the residues were located in the most preferred region, 6.0, 16.0, 32.0, 10.8, 4.8, and 9.5% in additional allowed region, 0.3, 1.3, 0.7, 2.2, 0.0, and 0.6% in generously A high degree of stereochemical quality of the model displays a score closing to 100%. ERRAT was used to assess the quality of the revised models. The AKT1, GDF-8, IGF-1, MyoD, and TNF- α scores were 92.877, 96.537, 92.972, 95.413, and 97.312, respectively, which is well within the usual range for a high grade model. The ProSA was used to generate the Z-score. The protein's Z score is represented by a single black point in this study (Figure 5). The Z-scores for AKT1, GDF-8, IGF-1, MuRF-1, MyoD, and TNF- were respectively -7.28, -4.98, -6.18, -5.9, -2.57, and -5.44 (Table 3). This demonstrated that the AKT1, GDF-8, IGF-1, MuRF-1, MyoD, and TNF-alpha structures were very dependable because their scores were well within the range generally reported for proteins of similar size to MyoD. In terms of energy function of amino acid residues, the quality of the protein folds of AKT1, GDF-8, IGF-1, MuRF-1, MyoD, and TNF- α models was also examined. Positive values, in general, correspond to problematic or incorrect parts of a model. Figure 3 shows that the MyoD's energy profile was compatible with a dependable conformation based on its resemblance to the AKT1, GDF-8, IGF-1, MuRF-1, and TNF-α.

Table 3: Validation of the AKT1, GDF-8, IGF-1, MuRF-1, MyoD and TNF-α proteins using PROCHECK, ProSA and Errat.

S. No.	Name of the proteins	Ramachandran plot statistics (%)				Z- scores	Overall protein factors
		Most favoured	*Additionally allowed*	*Generously allowed*	*Disallowed*		
1	AKT1	92.8	6.0	0.3	0.9	-7.28	92.877
2	GDF8/Myostatin	82.7	16.0	1.3	0.0	-4.98	96.537
3	IGF-1	67.3	32.0	0.7	0.0	-6.18	92.972
4	MuRF-1	85.8	10.8	2.2	1.2	-5.9	100.000
5	MyoD	95.2	4.8	0.0	0.0	-2.57	95.413
6	TNF-α	89.9	9.5	0.6	0.0	-5.44	97.312

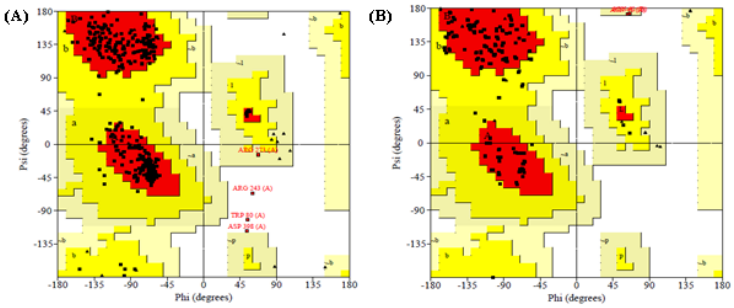

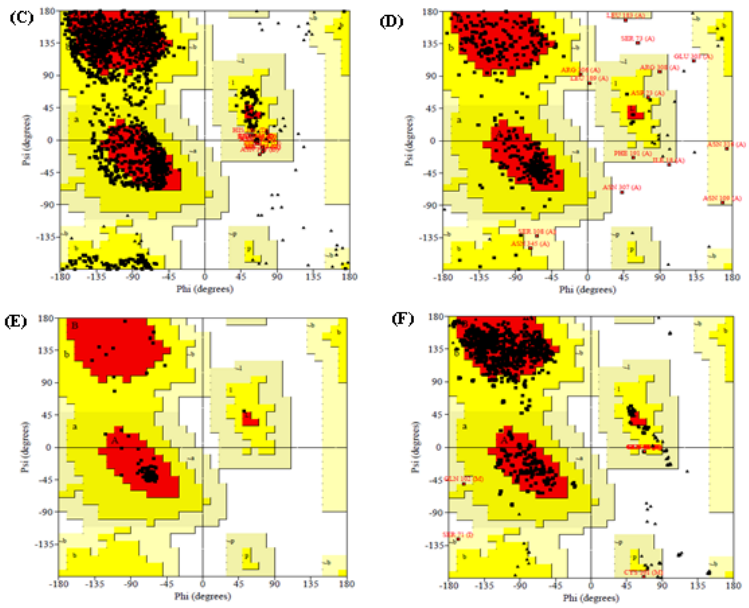

Figure 3: Ramachandran plots statistics (%) generated via (A) Akt1, (B) GDF-8, (C) IGF-1, (D) MuRF-1, (E) MyoD, and (F) TNF-α protein. PROCHECK displays the residues in the most preferred (red), additionally permitted (yellow), generously permitted (pale yellow), and disallowed regions.

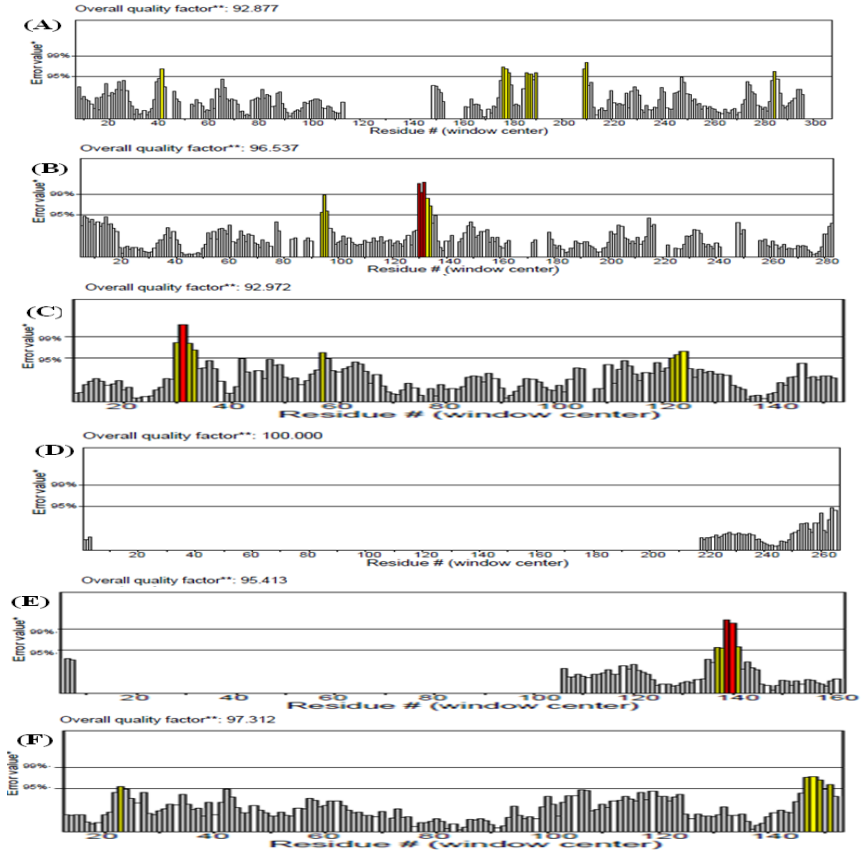

Figure 4: ERRAT plots for (A) Akt1, (B) GDF-8, (C) IGF-1, (D) MuRF-1, (E) myoD, and (F) TNF-α protein. The black bars represent the misfolded region located far from the active site; the grey bars represent the error region between 95% and 99%; and the white bars represent the region with a lower error rate for protein folding. * Two lines are drawn on the error axis to indicate the confidence with which regions that exceed that error value can be rejected. * The percentage of the protein whose calculated error value is less than the 95% rejection limit. Good high-resolution structures typically yield values of 95% or higher. The average overall quality factor for lower resolutions (2.5-3 A) is around 91%.

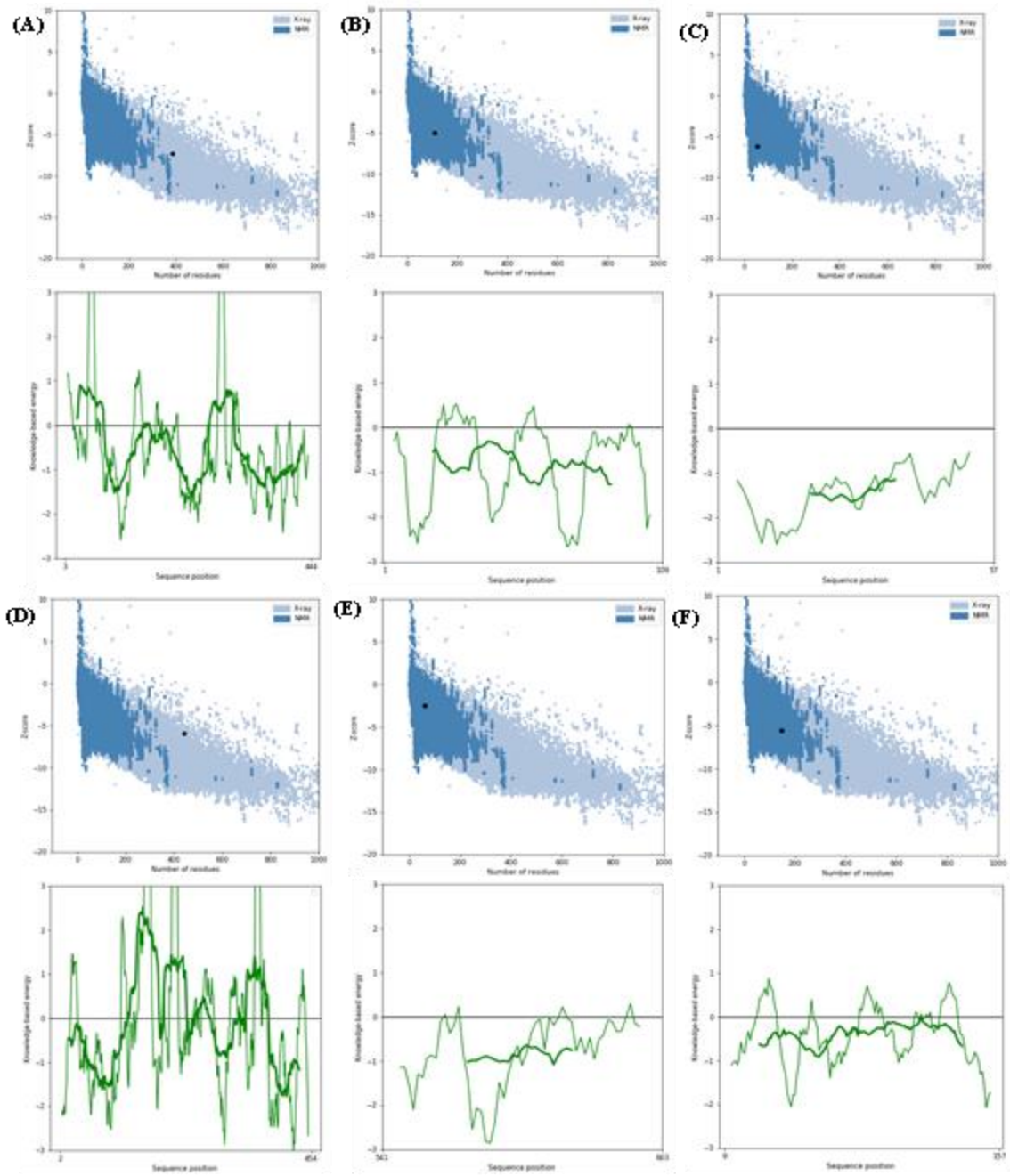

Figure 5: Protein quality scores for (A) Akt1, (B) GDF-8, (C) IGF-1, (D) MuRF-1, (E) MyoD, and (F) TNF-α protein generated through ProSA web server. The output shows Z-scores, which represent the general model quality, and energy plots, which represent the regional model quality. All protein chains in the PDB have their lengths determined by X-ray crystallography (light blue) and NMR spectroscopy (dark blue) using PROSA-web Z-scores. The large black dot denotes the range where the Z-score of protein models were present.

Ligand with protein interactions using Molecular docking studies

Docking studies predict binding interaction between ligand and its receptor (protein). AutoDock Vina is used to identify the binding properties of salbutamol with AKT1, GDF-8, IGF-1, MuRF-1, MyoD and TNF-α. The binding affinity and hydrogen bond of salbutamol to AKT1, GDF-8, IGF-1, MuRF-1, MyoD and TNF-α were -6.8, -5.8, -4.7, -6.1, -5.0 and -5.3kcal/mol and 1, 3, 2, 1, 2, and 1 (Table 4) respectively as measured by AutoDock Vina. These binding affinities were attributed to 1 or more hydrogen bond and 1 or more pi- alkyl bonds. The amino acids involved in the interaction of salbutamol and AKT1 include SER205, TRP80 and LEU264. The amino acids involved in the interaction of salbutamol l and MuRF1 include ALA:212, ASN:54, ASP:292, ARG:206, GLN:79, LEU:210, 213, 264, LYS:268, SER:205, TRP:80, TYR:263, 272, VAL:270; GDF-8 includes ALA:40, ASN:41, GLY:68, LEU:20, MET:79, 101, PHE:24, PRO:66, TYR:38, 42, VAL:22; IGF-1 includes CYS:18, GLN:15, GLY:19, PHE:16, 23, 25, TYR:24, VAL:17; Murf-1 includes ALA:321, ARG:169, 178, 323, ILE:322, GLN:167, 325, LEU:64, 180; MyoD includes ASN:560, ARG:564, 568, GLN:571, 580, GLY:567, ILE585, LYS:582, PHE:563; TNF-α includes GLN:61, 153, ILE:80, 118, LEU:94, PHE:152, SER:60, TRP:28, TYR:119, VAL:150 (Table 4). The complexes, along with the amino acids involved in binding are shown in Figure 6.

Table 4: Showing of the interactions of ligand (salbutamol) with different protein binding energies by autodocking

S. No.	Name of the proteins	Amino acids in interactions	Binding affinity (Kcal mol^{-1})	H-bond	Lipinski's rule of 5 for SLB	
					Properties	Values
1	AKT1	ALA:212, ASN:54, ASP:292, ARG:206, GLN:79, LEU:210, 213, 264, LYS:268, SER:205, TRP:80, TYR:263, 272, VAL:270.	-6.8	1	Molecular weight (<500Da)	239.311 g/mol
2	GDF8/ Myostatin	ALA:40, ASN:41, GLY:68, LEU:20, MET:79, 101, PHE:24, PRO:66, TYR:38, 42, VAL:22.	-5.8	3	H-band donor (≤5)	4
3	IGF-1	CYS:18, GLN:15, GLY:19, PHE:16, 23, 25, TYR:24, VAL:17.	-4.7	2	H-band acceptor (≤10)	4
4	MuRF-1	ALA:321, ARG:169, 178, 323, ILE:322, GLN:167, 325, LEU:64, 180.	-6.1	1		
5	MyoD	ASN:560, ARG:564, 568, GLN:571, 580, GLY:567, ILE585, LYS:582, PHE:563	-5.0	2	Log (p)	1.306
6	TNF-α	GLN:61, 153, ILE:80, 118, LEU:94, PHE:152, SER:60, TRP:28, TYR:119, VAL:150.	-5.3	1	Molar refractivity	66.745
					Violations	0

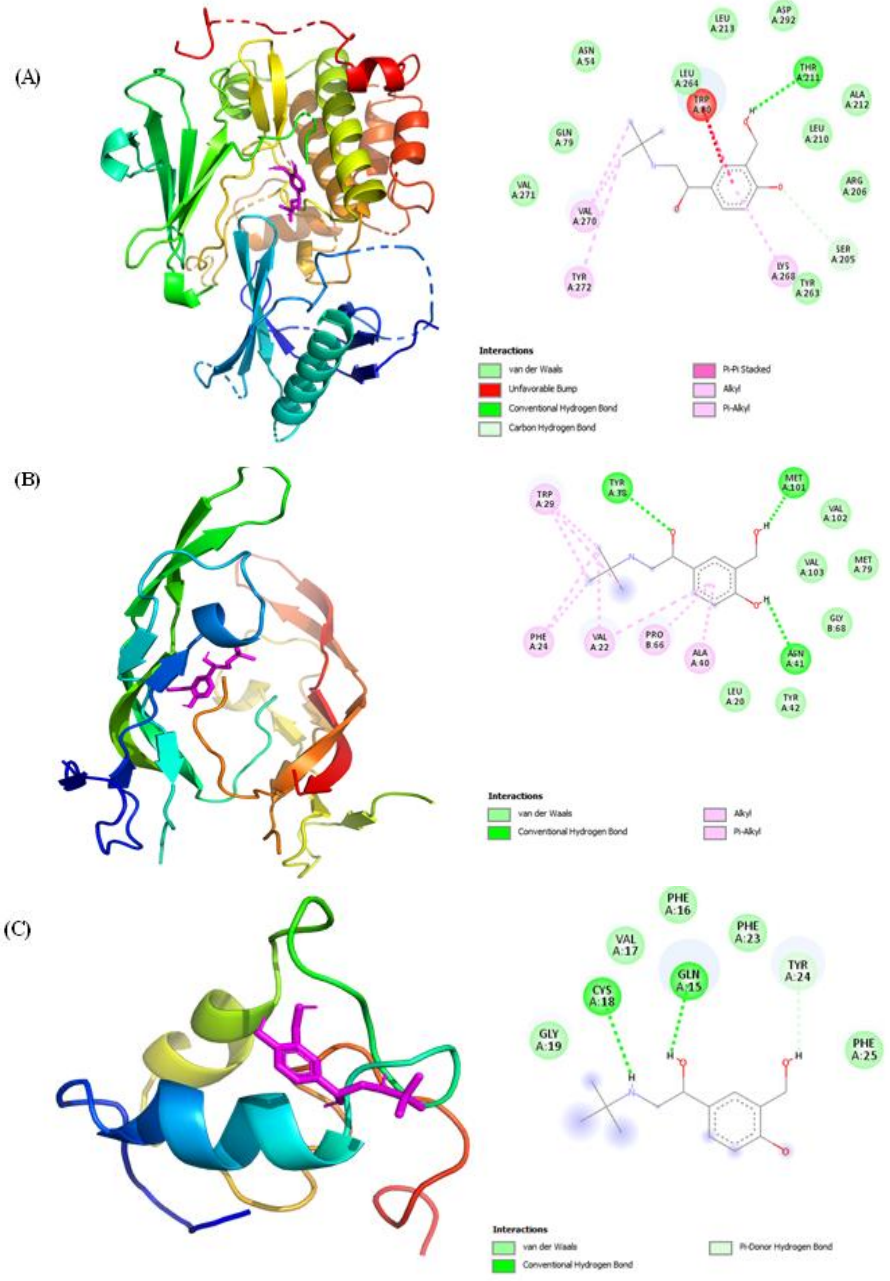

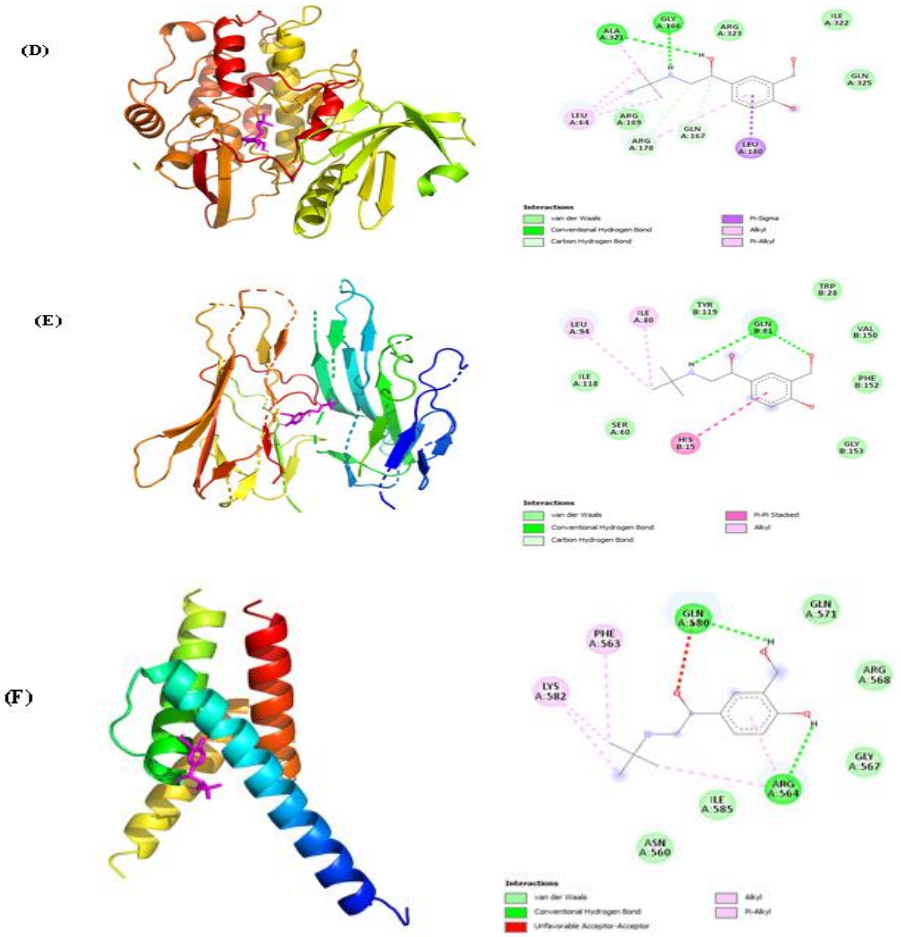

Figure 6: Representative interactions of ligand (salbutamol) with different proteins of the (A) 3D and 2D structure of Akt1, (B) 3D and 2D structure of GDF-8, (C) 3D and 2D structure of IGF-1, (D) 3D and 2D structure of MuRF-1, (E) 3D and 2D structure of MyoD, and (F) 3D and 2D structure of TNF-α generated by docking with help of PyMOL.

DISCUSSION

The current study used computational methods to estimate the protein-ligand interaction for receptor affinity in the beta 2-adrenergic agonist, salbutamol.

Further, results showed that salbutamol is having good solubility in distilled water, ether, 0.1N HCl, ethanol, and chloroform, as well as the associated and predicted values, were determined at 25° C. Visual examination revealed that the solubility of salbutamol increased with increasing concentrations of solvents such as distilled water, ether, 0.1N HCL, ethanol, and chloroform. This solubility pattern is found in many pharmaceutical nonelectrolytes and/or weak electrolyte drugs. Salbutamol has developed a model for predicting drug solubility in ionised or unionised solutions (Radivojev et al., 2021). At 276 nm, calibration curves for salbutamol were generated. At 225 nm, the overlapping UV-absorption spectra of salbutamol in ethanol. The calibration curve that resulted was linear, with a correlation coefficient (r^2) greater than 0.999. Because of this, the relationship between salbutamol concentrations and absorbance showed linearity and accuracy (Guo et al., 2016). The FTIR data revealed that there was no change in the spectra of pure salbutamol. The FTIR spectra of salbutamol revealed an intense absorption band at 1530.84 cm^{-1}, which corresponds to the presence of functional groups such as 1409 cm^{-1}, - (OH) for bending and Hydroxyl group, 1661 cm^{-1}, - (C=C) for stretching and aromatic ring, 1100 cm^{-1}, - (C-O) for stretching and ether group, 1028 cm^{-1}, - (C-H) for bending and aromatic Salbutamol's FTIR analysis shows no change in functional groups, confirming its undisturbed structure (Grisedale et al., 2013).

Following that, six protein models were examined using Ramachandran plot statistics analysis in PROCHECK by verifying the stereo-chemical quality of the protein structures on a residue-by-residue basis. A model with good stereo-chemical quality has a score close to 100%. As a result, the AKT1, GDF-8, IGF-1, MuRF-1, MyoD, and TNF-α models had acceptable stereo-chemical quality, with a low fraction of residues having phi/psi angles in the outlier zone. There were no poor connections or bad main chain or side chain parameter scores. AKT1, GDF-8, IGF-1, MuRF-1, MyoD, and TNF-α overall G factor values, on the other hand, were slightly out of range because they were less than -0.5. Acceptable G-factor values in PROCHECK range from 0 to -0.5, with values less than -0.5. In PROCHECK, acceptable G-factor values range from 0 to -0.5; values close to zero indicate the best quality models (Balaji et al., 2017).
ERRAT was used to assess the quality of the revised models. For non-bonded atomic interactions, ERRAT is also known as the "overall quality factor," with higher scores indicating higher quality. MuRF-1 had the highest ERRAT

score in this investigation, at 100%. (Figure 4). As a result, compared to previous protein models, MuRF-1 has a high resolution and quality. None of the residues exceeded the 99% error value limit (Balaji et al., 2017).
PROSA was utilised in this study to verify three-dimensional protein models for potential flaws. The Z-score reflects overall model quality and quantifies the structure's total energy departure from an energy distribution produced from random conformations. PROSA-web analysis revealed that, with the exception of some peaks in the middle region, the residue energy of the AKT1, GDF-8, IGF-1, MuRF-1, and TNF-α model was largely negative (Balaji et al., 2017).
The availability of predicted protein structures for entire proteomes could enable the identification of molecular drug targets and drug mechanisms of action, which is an important use case for protein structure predictions. Now, we used molecular docking simulations to predict protein-ligand interactions for anti-atrophy. To predict protein-ligand interactions, we combined protein structure predictions with docking. We discovered that this method accurately predicts widespread promiscuity compounds and essential protein targets, as well as known 2-adrenergic agonists and salbutamol-protein interactions, with weak to moderate true-positive rates depending on the stringency of the binding affinity threshold used (Wang et al., 2020).

CONCLUSIONS

These findings suggested that a computational approach could be used to predict skeletal muscle atrophy by combining AKT1, GDF-8, IGF-1, MuRF-1, MyoD, and TNF-alpha with the beta 2-adrenergic agonist salbutamol.

Conflict of interest

Authors declare no conflicts of interest.

Acknowledgement

The authors are grateful to the Babasaheb Bhimrao Ambedkar University, Lucknow, India, for providing the required infrastructure for the study

Funding

This work was supported by University Grants Commission (UGC) startup grant (F. 30–460/2019 (BSR) to Dr. Sapana Kushwaha and Indian Council of Medical Research-Senior Research Fellowship (ICMR-SRF) (File no-3/1/3/8/Dis & Rehab/2022-NCD-II) to Anand Kumar.

Data availability statement

The data that support the findings of this study are available on request from the corresponding author.

REFERENCES

1. Balaji, G. A., Nagendra, H. G., Balaji, V. N., & Rao, S. N. (2017). Experimental conformational energy maps of proteins and peptides. Proteins, 85(6), 979-1001. https://doi.org/10.1002/prot.25266
2. Cohen, S., Nathan, J. A., & Goldberg, A. L. (2015). Muscle wasting in disease: molecular mechanisms and promising therapies. Nat Rev Drug Discov, 14(1), 58-74. https://doi.org/10.1038/nrd4467
3. Costanzi, S., & Vilar, S. (2012). In silico screening for agonists and blockers of the β(2) adrenergic receptor: implications of inactive and activated state structures. J Comput Chem, 33(5), 561-572. https://doi.org/10.1002/jcc.22893
4. Elfellah, M. S., Dalling, R., Kantola, I. M., & Reid, J. L. (1989). Beta-adrenoceptors and human skeletal muscle characterisation of receptor subtype and effect of age. Br J Clin Pharmacol, 27(1), 31-38. https://doi.org/10.1111/j.1365-2125.1989.tb05332.x
5. Galaz-Montoya, M., Wright, S. J., Rodriguez, G. J., Lichtarge, O., & Wensel, T. G. (2017). β(2)-Adrenergic receptor activation mobilizes intracellular calcium via a non-canonical cAMP-independent signaling pathway. J Biol Chem, 292(24), 9967-9974. https://doi.org/10.1074/jbc.M117.787119
6. Grisedale, L. C., Moffat, J. G., Jamieson, M. J., Belton, P. S., Barker, S. A., & Craig, D. Q. (2013). Development of photothermal FTIR microspectroscopy as a novel means of spatially identifying amorphous and crystalline salbutamol sulfate on composite surfaces. Mol Pharm, 10(5), 1815-1823. https://doi.org/10.1021/mp300605s
7. Guo, Z., Chen, Y., Ding, X., Huang, C., & Miao, L. (2016). Simultaneous determination of ambroxol and salbutamol in human plasma by ultra-performance liquid chromatography-tandem mass spectrometry and its application to a pharmacokinetic study. Biomed Chromatogr, 30(11), 1789-1795. https://doi.org/10.1002/bmc.3754
8. Hostrup, M., Reitelseder, S., Jessen, S., Kalsen, A., Nyberg, M., Egelund, J., Kreiberg, M., Kristensen, C. M., Thomassen, M., Pilegaard, H., Backer, V., Jacobson, G. A., Holm, L., & Bangsbo, J. (2018). Beta(2) -adrenoceptor agonist salbutamol increases protein turnover rates and alters signalling in skeletal muscle after resistance exercise in young men. J Physiol, 596(17), 4121-4139. https://doi.org/10.1113/jp275560
9. Meng, X. Y., Zhang, H. X., Mezei, M., & Cui, M. (2011). Molecular docking: a powerful approach for structure-based drug discovery. Curr Comput Aided Drug Des, 7(2), 146-157. https://doi.org/10.2174/157340911795677602
10. Morissette, M. R., Cook, S. A., Buranasombati, C., Rosenberg, M. A., & Rosenzweig, A. (2009). Myostatin inhibits IGF-I-induced myotube hypertrophy through Akt. Am J Physiol Cell Physiol, 297(5), C1124-1132. https://doi.org/10.1152/ajpcell.00043.2009
11. Pijet, B., Pijet, M., Litwiniuk, A., Gajewska, M., Pająk, B., & Orzechowski, A. (2013). TNF- α and IFN-s-dependent muscle decay is linked to NF-κB and STAT-1α-stimulated Atrogin1 and MuRF1 genes in C2C12 myotubes. Mediators Inflamm, 2013, 171437. https://doi.org/10.1155/2013/171437
12. Radivojev, S., Luschin-Ebengreuth, G., Pinto, J. T., Laggner, P., Cavecchi, A., Cesari, N., Cella, M., Melli, F., Paudel, A., & Fröhlich, E. (2021). Impact of simulated lung fluid components on the solubility of inhaled drugs and predicted in vivo performance. Int J Pharm, 606, 120893. https://doi.org/10.1016/j.ijpharm.2021.120893
13. Sartori, R., Romanello, V., & Sandri, M. (2021). Mechanisms of muscle atrophy and hypertrophy: implications in health and disease. Nat Commun, 12(1), 330. https://doi.org/10.1038/s41467-020-20123-1
14. Savjani, K. T., Gajjar, A. K., & Savjani, J. K. (2012). Drug solubility: importance and enhancement techniques. ISRN Pharm, 2012, 195727. https://doi.org/10.5402/2012/195727
15. Wang, P., Wang, L., Peng, Z., & Fu, Z. (2020). Flow microdialysis sampling-chemiluminescent detection coupled with molecular docking for the investigation of binding behavior between salbutamol and DNA. Talanta, 208, 120367. https://doi.org/10.1016/j.talanta.2019.120367

16. Yoshida, T., & Delafontaine, P. (2020). Mechanisms of IGF-1-Mediated Regulation of Skeletal Muscle Hypertrophy and Atrophy. Cells, 9(9). https://doi.org/10.3390/cells9091970